Inflammation, Vol. 40, No. 6, December 2017 (© 2017)
DOI: 10.1007/s10753-017-0632-3

ORIGINAL ARTICLE

Necrostatin-1 Protects Against D-Galactosamine and Lipopolysaccharide-Induced Hepatic Injury by Preventing TLR4 and RAGE Signaling

Seok-Joo Kim[1] and Sun-Mee Lee[1,2]

Abstract— Fulminant hepatic failure (FHF) is a life-threatening clinical syndrome results in massive inflammation and hepatocyte death. Necroptosis is a regulated form of necrotic cell death that is emerging as a crucial control point for inflammatory diseases. The kinases receptor interacting protein (RIP) 1 and RIP3 are known as key modulators of necroptosis. In this study, we investigated the impact of necroptosis in the pathogenesis of FHF and molecular mechanisms, particularly its linkage to damage-associated molecular pattern (DAMP)-mediated pattern recognition receptor (PRR) signaling pathways. Male C57BL/6 mice were given an intraperitoneal injection of necrostatin-1 (Nec-1, RIP1 inhibitor; 1.8 mg/kg; dissolved in 2% dimethyl sulfoxide in phosphate-buffered saline) 1 h before receiving D-galactosamine (GalN; 800 mg/kg)/lipopolysaccharide (LPS; 40 μg/kg). Hepatic RIP1, RIP3 protein expression, their phosphorylation, and RIP1/RIP3 complex formation upregulated in the GalN/LPS group were attenuated by Nec-1. Nec-1 markedly reduced the increases in mortality and serum alanine aminotransferase activity induced by GalN/LPS. Increased serum high mobility group box 1 (HMGB1) and interleukin (IL)-33 release, HMGB1-toll-like receptor 4 and HMGB1-receptor for advanced glycation end products (RAGE) interaction, and nuclear protein expressions of NF-κB and early growth response protein-1 (egr-1) were attenuated by Nec-1. Our finding suggests that necroptosis is responsible for GalN/LPS-induced liver injury through DAMP-activated PRR signaling.

KEY WORDS: damage-associated molecular pattern; fulminant hepatic failure; inflammation; necrostatin-1.

INTRODUCTION

Fulminant hepatic failure (FHF) is a dramatic clinical syndrome that results from massive hepatocyte death. FHF has a variety of causes, such as hepatitis virus infection, toxic insult, autoimmunity, liver transplantation, drugs, or ischemia/reperfusion (I/R) and there is no effective therapy for disease clinically other than liver transplantation [1]. A model of D-galactosamine (GalN)/lipopolysaccharide (LPS)-induced acute liver failure is widely used to explore the mechanism of FHF, as it demonstrates an inflammation-mediated hepatocellular injury process, resulting from hepatocellular necrosis and apoptosis. Although the nature of FHF has been extensively studied, the molecular pathways by which hepatocellular damage occurs are not fully understood.

Recently, a novel mechanism called "programmed necrosis" or necroptosis has been suggested as important mediator of cell death. Necroptosis incorporates features of apoptosis and necrosis. Necroptosis shares upstream molecular machinery with apoptosis, and the

[1] School of Pharmacy, Sungkyunkwan University, Suwon, 16419, Republic of Korea
[2] To whom correspondence should be addressed at School of Pharmacy, Sungkyunkwan University, Suwon, 16419, Republic of Korea. E-mail: sunmee@skku.edu

final outcome of necroptosis is cellular leakage as a result of organelle and cellular swelling, which is morphological characteristics of necrosis [2]. Necroptosis is typically initiated *via* death receptors, such as Fas or tumor necrosis factor (TNF) receptors. Receptor interacting proteins (RIPs) are essential for necroptosis execution; for pronecrotic complex formation, the kinase activities of RIP1 and RIP3 are essential and are tightly regulated within the necrosome, a key transducer of necroptotic signal [3]. The discovery of necrostatin-1 (Nec-1) as RIP1-specific kinase inhibitor enabled selective inhibition of necroptosis and investigation of its contribution to pathophysiological conditions [4]. Nec-1 showed a significant protection against excitotoxicity in primary rat cortical culture and in a mouse hippocampal cell, as well as myocardial I/R model, suggesting a mechanistic involvement of RIP1 kinase in various inflammatory diseases [5–7]. Recently, several studies reported the evidence of protective effects achieved through inhibition of necroptosis or treatment necrostatins in liver-related disease conditions, particularly in concanavalin A (Con A)-induced hepatitis [8–11]. Furthermore, Nec-1 treatment or genetic ablation of RIP3 reduced hepatocellular damage against acetaminophen intoxication [12, 13], but their molecular pathogenesis in liver inflammation remains unclear in GalN/LPS-induced liver failure.

Necroptosis leads to rapid plasma membrane permeabilization and to the release of cell contents and exposure of damage-associated molecular patterns (DAMPs). Studies performed on tubular epithelial cells and the kidney allograft animals showed increased high mobility group box 1 (HMGB1) releases, which were attenuated in genetic deletion of RIP3 [14]. Moreover, RIP3 promoted a retinal inflammatory response by releasing HMGB1 after poly(I:C) injection [15]. RIP1 and RIP3 have key roles in controlling the outcome of death receptor signaling pathways, but they also have important roles in pattern recognition receptors (PRRs) pathways. Stimulation of Toll-like receptor 4 (TLR4) by LPS in combination with caspase inhibitor leads to RIP3-mediated necroptosis in murine macrophages [16]. Necroptotic DAMPs can contribute to sensitization of necroptosis in neighboring cells *via* induction of PRRs [17]. Necroptotic DAMPs have associated with inflammatory diseases; however, the precise mechanisms and role of DAMPs in immune responses remain unknown. This study investigated the molecular mechanisms behind necroptosis activation and signaling pathways associated with GalN/LPS-induced hepatic inflammation.

MATERIALS AND METHODS

Animals and Drug Treatment

Male C57BL/6 mice (20–22 g) were fasted overnight but were given access to water *ad libitum*. All animal experiments were approved by the Animal Care Committee of Sungkyunkwan University School of Pharmacy (SUSP14-05) and performed in accordance with the guidelines of National Institutes of Health (NIH publication No.86-23, revised 1985). All animals (except for normal controls) were injected intraperitoneally with GalN (800 mg/kg; Sigma-Aldrich, USA) and LPS (40 μg/kg *Escherichia coli* O26: B6; Sigma-Aldrich) dissolved in phosphate-buffered saline. Nec-1 (Millipore, USA) was dissolved in 2% dimethyl sulfoxide in phosphate-buffered saline. Mice were treated intraperitoneally with Nec-1 at 1 h before GalN/LPS challenge. The dose and the injection time of Nec-1 treatment were selected according to previous reports and our preliminary study [9]. Mice were randomly divided into four groups: (a) vehicle-treated control, (b) Nec-1-treated control, (c) vehicle-treated GalN/LPS, and (d) Nec-1 1.8 mg/kg-treated GalN/LPS.

Determination of Lethality

Animals were monitored until they met criteria for euthanasia or 24 h following GalN/LPS challenge. The numbers of dead mice were counted at 6, 8, 10, 12, 18, and 24 h after GalN/LPS injection.

Serum Alanine Aminotransferase (ALT) Activity and HMGB1, IL-33 Levels

The blood sample was collected and then ALT activity was determined by standard spectrophotometric procedures using Chemi-Lab ALT assay kits (IVD Lab, Republic of Korea). The serum cytokine levels were quantified with an enzyme-linked immunosorbent assay (ELISA) with a commercial mouse HMGB1 (Chondrex, USA) and IL-33 (eBioscience, USA) ELISA kit according to the manufacturer's instruction.

Histological Analysis

Liver tissue was removed from a portion of the left lobe, fixed immediately in 10% neutral-buffered formalin, embedded in paraffin, and serially cut into 5-μm-thick sections. The hematoxylin and eosin-stained sections were evaluated using an optical microscope (Olympus Optical, Tokyo, Japan). The histological changes were evaluated at ×200 magnification by a point-counting method for

severity of hepatic injury using an ordinal scale. The stained sections were graded as follows: grade 0, minimal or no evidence of injury; grade 1, mild injury with cytoplasmic vacuolation and focal nuclear pyknosis; grade 2, moderate to severe injury with extensive nuclear pyknosis, cytoplasmic hypereosinophilia, and loss of intercellular borders; and grade 3, severe necrosis with disintegration of hepatic cords, hemorrhage, and neutrophil infiltration.

Total RNA Isolation and Quantitative Real-Time RT-PCR Analysis

For mRNA analysis, total RNA was first extracted from the liver tissue of different treatment groups using RNAiso Plus (Takara, Japan). cDNA was synthesized using a reverse transcription reaction (EcoDry™ cDNA Synthesis Premix, Takara). The cDNA was amplified using real-time PCR with a thermocycler (Lightcycler® Nano, Roche Applied Science, Germany) and SYBR Green detection system. The gene-specific primers used for amplification of cDNA are as follows. *RIP1*: 5′-GAAGACAGACCTAGACAGCGG -3′ (sense), 5′-CAGTAGCTTCACCACTCGAC -3′ (antisense), *RIP3*: 5′- CAGTGGGACTTCGTGTCCG -3′ (sense), 5′-AAGCTGTGTAGGTAGCACATC -3′ (antisense), *β-actin*: 5′- TGGAATCCTGTGGCATCCAT -3′ (sense), and 5′- TAAAACGCAGCTCAGTAACA -3′ (antisense). The mRNA expression levels of genes were normalized to the expression level of the β-actin and relative to the average of all delta C_t-values in each sample using the cycle threshold (C_t) method.

Preparation of Protein Extracts and Western Blot Immunoassay

Fresh liver tissue was isolated and homogenized in PRO-PREP® (Intron, Republic of Korea) for whole protein samples and in NE-PER® (Thermo-Fisher, USA) for extraction of cytosolic protein samples. Proteins (20 μg) were loaded onto 10% polyacrylamide gels for electrophoresis, then transferred to nitrocellulose membranes. Bands were detected immunologically using polyclonal antibodies against mouse RIP1 (1:5000), phospho-RIP1 (1:5000; BD Biosciences, USA), RIP3 (1:5000), phospho-RIP3 (1:5000; Santa Cruz, USA), phosphoserine (1:2500), phospho-MLKL (p-MLKL, 1:4000; Santa Cruz), HMGB1 (1:4000; Abcam, USA), TLR2, TLR4, TLR9 (1:4000; Santa Cruz), RAGE (1:2500; Abcam), NF-κB, early growth response protein 1 (egr-1), and chemokine (C-X-C motif) ligand 2 (CXCL2; 1:4000; Abcam). Monoclonal antibody against mouse β-actin (Sigma-Aldrich) was used as a loading control. The binding of all antibodies was detected using an ECL detection system and analyzed using a densitometric analysis software.

Co-immunoprecipitation and Immunoblotting

Whole cell lysates were incubated overnight with mouse anti-RIP1 antibody (1:100; BD Biosciences), anti-RIP3 antibody (1:100; Santa Cruz), anti-TLR4 antibody (1:100; Santa Cruz), anti-RAGE antibody (1:100; Abcam), and anti-HMGB1 antibody (1:100; Abcam). The immune complexes were then precipitated *via* incubation with protein A/G-agarose beads (Santa Cruz) for 6 h followed by extensive washing with a radioimmunoprecipitation assay buffer. Immunoprecipitated proteins were eluted with 2× sodium dodecyl sulfate (SDS) loading buffer, separated using SDS gels, and transferred onto a nitrocellulose membrane where the immunoblot was processed.

Immunohistochemistry (IHC) Staining

Hepatic tissue samples were re-fixated in 10% NBF and then embedded in paraffin, sectioned (4 μm), and stained with ABC-based IHC methods for an apoptotic marker, cleaved caspase-3. The changes of cleaved caspase-3 immunoreactive cells on the liver section were observed using purified primary antibody (anti-cleaved caspase-3 antibody; Cell Signaling Technology Inc., Beverly, USA; 1:400) with ABC and peroxidase substrate kit (Vector Labs, Burlingame, CA, USA). Briefly, endogenous peroxidase activity was blocked by incubated in methanol and 0.3% H_2O_2 for 30 min, and non-specific binding of immunoglobulin was blocked with normal horse serum blocking solution for 1 h in humidity chamber after heating (95–100 °C)-based epitope retrievals in 10 mM citrate buffers (pH 6.0). Primary antisera were treated for overnight at 4 °C in humidity chamber and then incubated with biotinylated universal secondary antibody and ABC reagents for 1 h at room temperature in humidity chamber. Finally, sections were reacted with peroxidase substrate kit for 3 min at room temperature. All sections were rinsed in 0.01 M PBS for three times, between each step. The cells occupied by over 20% of immunoreactivities, the density, of cleaved caspase-3 as compared to background, were regarded as positive in this study, and the numbers of cleaved caspase-3 immunolabeled cells located in frame of view were calculated using a computer-based automated image analyzer (iSolution^{FL} 9.1, IMT i-solution Inc., Vancouver, Canada) under a light microscope (Model Eclipse 80i, Nikon, Tokyo, Japan), among total 1000 hepatocytes (cells/1000 hepatocytes).

Statistical Analysis

Results are expressed as mean ± S.E.M. Survival data were analyzed with Kaplan-Meier curves and the log-rank test. All other data were analyzed by two-way analysis of variance (ANOVA). The differences between groups were considered significant at the $P < 0.05$ level after the appropriate Bonferroni correction was performed for multiple comparisons.

RESULTS

GalN/LPS Induces Necroptosis

Hepatic RIP1 and RIP3 mRNA and protein expressions increased 1 h after GalN/LPS injection and remained increased at 3, 6, 12, and 24 h of GalN/LPS challenge, but increase of RIP1 and RIP3 expressions were attenuated by Nec-1 treatment at both 3 and 6 h after GalN/LPS injection (data not shown). To examine whether expressed RIP1 and RIP3 interact and form necrosome after GalN/LPS injection, co-immunoprecipitation was conducted. Furthermore, the phosphorylation of RIP1 and RIP3 is an essential process resulting in stable assembly of pronecrotic RIP1-RIP3 complex, and thus, phosphoserine contents were measured. The phosphoserine content and RIP3 protein immunoprecipitated with RIP1-specific antibody was significantly increased 3 h after GalN/LPS injection (2.2- and 4.4-fold *vs.* control, respectively; Fig. 1a). After 3 h of GalN/LPS injection, the phosphoserine content and RIP1 protein immunoprecipitated with RIP3-specific antibody were significantly increased (1.8- and 2.4-fold *vs.* control, respectively; Fig. 1a). These changes are attenuated in animals received Nec-1. As shown in Fig. 1b, hepatic p-MLKL level was increased after 3 h of GalN/LPS injection, but attenuated by Nec-1 pretreatment. After 3 h of GalN/LPS injection, cleaved caspase-3 immunoreactive hepatocyte numbers were significantly increased, but Nec-1 pretreatment attenuated these increases (Fig. 1c).

Nec-1 Attenuated GalN/LPS-Induced Lethality and Hepatocellular Damage

By pretreatment with Nec-1, we first aimed to define the role of RIP1 inhibition on GalN/LPS-induced FHF in animals. In the GalN/LPS group, mice began to die 6 h after GalN/LPS injection. The survival rate was 50% at 6 h and reached 10% 12 h after D-GalN/LPS injection. However, treatment with Nec-1 reduced the mortality significantly ($p = 0.0052$; Fig. 2a). The serum level of ALT, a marker of hepatocellular injury, was 39.2 ± 6.2 U/L in the control group. After 3 h of GalN/LPS injection, ALT level significantly increased to 306.2 ± 96.0 U/L, and this increase was attenuated by Nec-1 (Fig. 2b). The histological features shown in Fig. 2c indicate a normal liver lobular architecture and cell structure in the livers of control animals. Three hours after GalN/LPS, marked histopathologic changes occurred in the liver (inflammatory cell infiltration, portal inflammation, and hepatocellular necrosis). These were ameliorated in animals that received Nec-1.

GalN/LPS-Induced Serum Releases of DAMPs Are Ameliorated by Nec-1 Administration

After GalN/LPS challenge, we observed severe hepatocellular death at 3 h. We utilized ELISA to assess endogenous DAMPs released after cell death. In control animals, serum levels of HMGB1 and IL-33 were low. Serum HMGB1 and IL-33 levels increased significantly to 7.4 ± 0.7 ng/ml and 43.1 ± 10.1 pg/ml at 3 h after GalN/LPS treatment, and 9.7 ± 1.1 and 32.9 ± 7.1 pg/ml at 6 h after GalN/LPS treatment, respectively. Nec-1 attenuated these increases (Fig. 3).

Nec-1 Attenuated Hepatic Protein Expression of TLR4 and RAGE, But Did Not Affect TLR2 and TLR9

Since TLRs and RAGE are PRRs that recognize DAMPs, we investigated the effect of Nec-1 pretreatment on PRR expression after GalN/LPS challenge. Hepatic TLR2, TLR4, TLR9, and RAGE protein expressions after 3 h of GalN/LPS injection are shown in Fig. 3. The level of hepatic TLR2, TLR4, TLR9, and RAGE protein expressions were significantly increased at 3 h after GalN/LPS injection (TLR2; 3.1-fold, TLR4; 4.2-fold, TLR9; 2.0-fold, RAGE; 2.6-fold *vs.* control, respectively). Nec-1 attenuated the increase of hepatic TLR4 and RAGE protein expression, while it did not affect the hepatic TLR2 and TLR9 protein expression.

GalN/LPS-Induced Interaction of HMGB1 on PRR Is Attenuated After Nec-1 Pretreatment

In addition to hepatic TLR4 and RAGE expression, the interaction between HMGB1 and PRRs is responsible for amplifying the inflammatory response in the liver during FHF. Therefore, in HMGB1 with TLR4 and RAGE, co-immunoprecipitations were conducted in whole liver tissues. Three hours after GalN/LPS challenge, there was a significant increase in TLR4 and RAGE contents in the complexes immunoprecipitated with HMGB1-specific

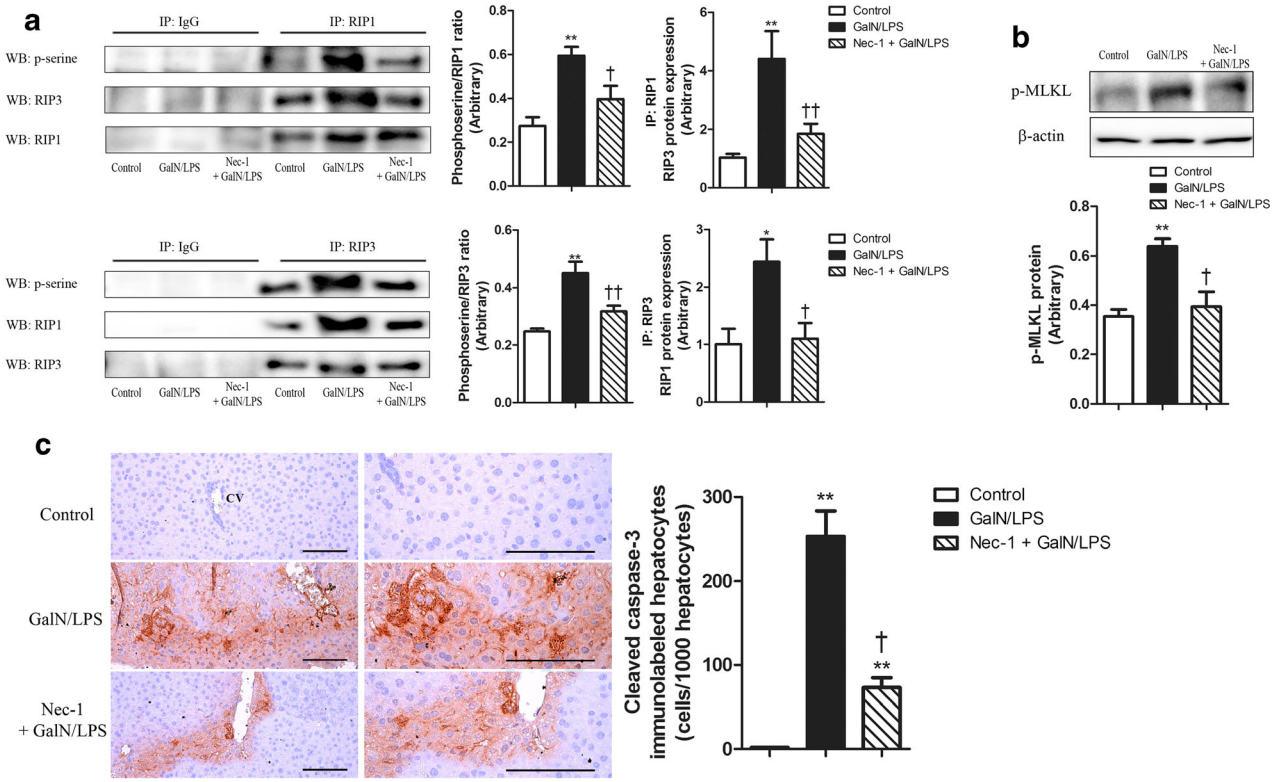

Fig. 1. Nec-1 attenuates hepatic GalN/LPS-induced necroptosis. **a** RIP1-RIP3 necrosome formation and RIP1 and RIP3 phosphorylation. **b** Hepatic p-MLKL protein level was measured. **c** Immunohistochemistry of mouse liver against GalN/LPS injection. Cleaved caspase-3 was stained and immunolabeled hepatocytes are quantified. The cells occupied by over 20% of immunoreactivities, the density, against cleaved caspase-3 as compared to background were regarded as positive, and the numbers of cleaved caspase-3 immunolabeled cells on liver section were calculated by a computer-based automated digital image analyzer among total 1000 hepatocytes under a light microscope as blinds to group distribution when this analysis was made. *Scale bars* = 100 μm. *CV* central vein. Mice were treated intraperitoneally with Nec-1 (1.8 mg/kg) or vehicle (2% DMSO in phosphate-buffered saline) at 1 h before GalN (800 mg/kg)/LPS (40 μg/kg) challenge. The results are presented as mean ± S.E.M. of 8 to 10 animals per group. The *asterisks* denote significant differences (*$P < 0.05$, **$P < 0.01$) *versus* the control group. The *dagger signs* denote significant differences ($^{\dagger}P < 0.05$, $^{\dagger\dagger}P < 0.01$) *versus* the GalN/LPS group.

antibody. Furthermore, HMGB1 contents in the complexes immunoprecipitated with TLR4 and RAGE-specific antibody were increased at 3 h after GalN/LPS injection. However, pretreatment of Nec-1 attenuated these changes (Fig. 4).

GalN/LPS-Induced Inflammatory Transcription Factor Activation and CXCL2 Production Were Attenuated by Nec-1 Treatment

The key inflammatory transcription factor NF-κB and egr-1 are responsible for expression of various genes crucial in the development of acute inflammation. To determine whether stimulation of PRR signals initiated inflammatory response, the protein levels of the transcription factors in the nuclear extracts from liver tissues have been assessed. At 3 h after GalN/LPS injection, nuclear NF-κB p65 and egr-1 protein markedly increased by 1.8- and 2.1-fold of the control, respectively. Nec-1 attenuated these increases. We assessed the production of CXCL2, which is central downstream gene of egr-1 upregulation and drives chemotaxis of neutrophils after sterile liver injury [18]. Hepatic CXCL2 expression upregulated by 3.1-fold *vs*. control after 3 h after GalN/LPS treatment, and Nec-1 treatment attenuated these increases (Fig. 5).

DISCUSSION

Necroptotic cell death has role in the host response to viral and bacterial infection [19], as well as the pathogenesis of TNF-induced sterile septic shock [20]. There is a direct association between cell death and progression of FHF; however, differential contribution of specific cell death pathways to hepatocyte injury during FHF is still

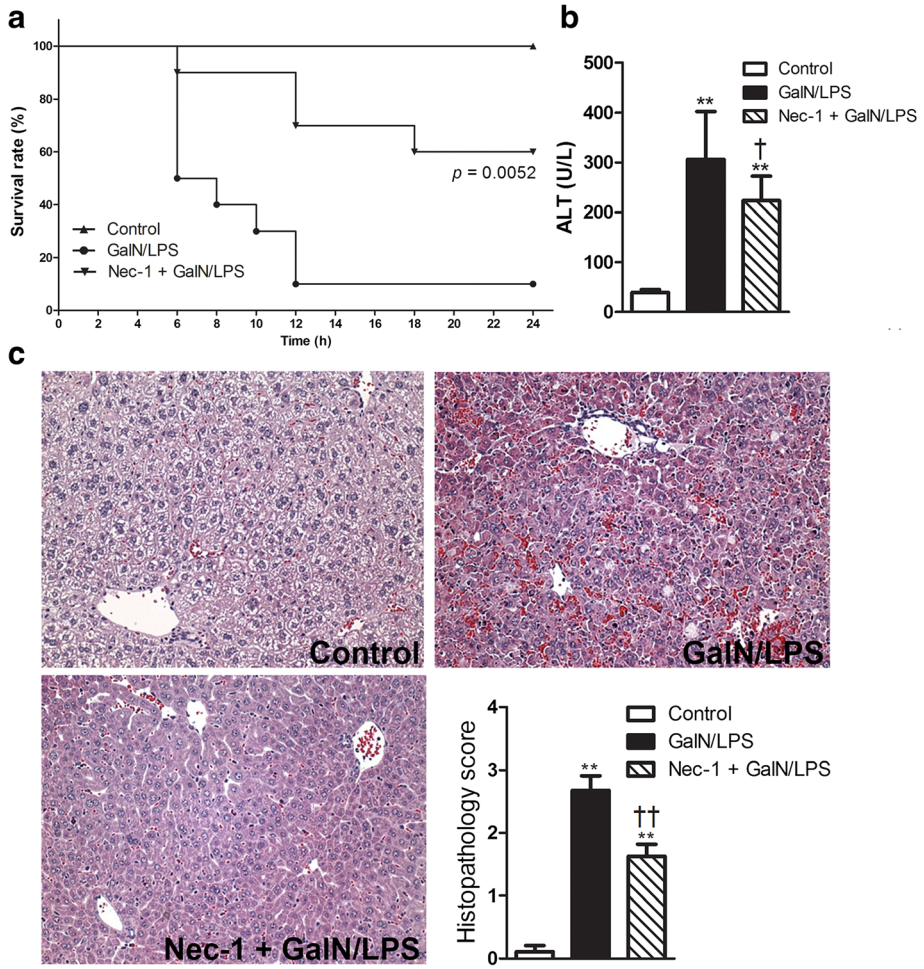

Fig. 2. Nec-1 attenuates GalN/LPS-induced mortality and liver injury. **a** Mice were given intrapenitoneal Nec-1 (1.8 mg/kg) or vehicle (2% DMSO) before 1 h of GalN (800 mg/kg)/LPS (40 μg/kg) injection. Mice were monitored for 24 h for survival. The results of treatment groups were compared with those of the vehicle (2% DMSO)-treated GalN/LPS group. $N = 10$ per group. **b** Serum ALT levels are presented as mean ± S.E.M. of 8 to 10 animals per group. **c** Histological micrographs of liver tissues stained with hematoxylin and eosin are shown (magnification ×200). The results are presented as mean ± S.E.M. of 8 to 10 animals per group. The *asterisk* denotes significant differences (**$P < 0.01$) *versus* the control group. The *dagger signs* denote significant differences ($^{\dagger}P < 0.05$, $^{\dagger\dagger}P < 0.01$) *versus* the GalN/LPS group.

not understood. When apoptosis is prevented by pharmacological intervention, GalN/LPS-induced liver injury still progresses in mouse models [21]. These data suggest that nonapoptotic cell death pathways are critical for hepatocyte death following GalN/LPS administration.

Many studies have proved that necroptosis is a highly regulated form of cell death pathway involved in the intracellular assembly of necrosome [22]. This process is triggered by a number of different receptors such as TNF receptor, TLR, or T cell receptor. In detail, in response to upstream signal, RIP1 is activated, and its phosphorylation and oligomerization lead to the functional interplay between RIP1 and RIP3. RIP3 activation results in the phosphorylation and oligomerization of MLKL, which is considered as a possible terminal necroptotic effector by triggering the disruption of cellular membranes to cause cell lysis [23, 24]. In the present study, GalN/LPS induced RIP1 and RIP3, central molecules of the necroptotic pathway. Furthermore, we observed a significant increase in RIP1, RIP3, RIP phosphorylation, and association between RIP1 and RIP3 after GalN/LPS injection. We detected increase in p-MLKL after GalN/LPS challenge, which is in accordance with previously published report of non-alcoholic fatty liver disease [25]. Treatment with a RIP1 kinase inhibitor, Nec-1, blocked RIP phosphorylation and formation of RIP1-RIP3 complex. Concomitantly, Nec-1 improved increased

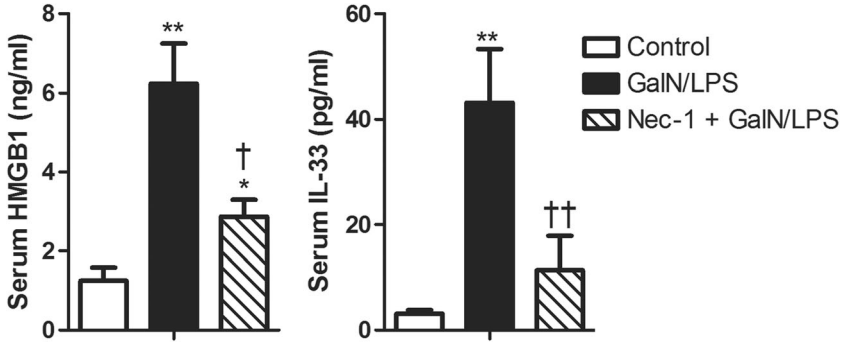

Fig. 3. Nec-1 attenuates GalN/LPS-induced increases in serum HMGB1 and IL-33 releases. Mice were given intrapenitoneal Nec-1 (1.8 mg/kg) or vehicle (2% DMSO) before 1 h of GalN (800 mg/kg)/LPS (40 μg/kg) injection. Serum samples were obtained 3 h after GalN/LPS injection. The results are presented as mean ± S.E.M. of 8 to 10 animals per group. The *asterisks* denote significant differences (*$P < 0.05$, **$P < 0.01$) from the control group. The *dagger signs* denote significant differences ($^{\dagger}P < 0.05$, $^{\dagger\dagger}P < 0.01$) from the GalN/LPS group.

lethality after GalN/LPS injection and attenuated the increase of serum levels and hepatocellular damages evidenced by histological observations. These results indicate that RIP1/3-driven necroptosis is responsible for hepatocellular injury induced by GalN/LPS, and these alterations are attenuated by pharmacological inhibition of RIP1.

However, it should be noted that necroptosis is not the only cell death involved in GalN/LPS injury. Previous studies showed that LPS-induced cell death in GalN-sensitized mice is driven by TNF-α [26, 27] and transduces predominantly apoptosis signals though TNF/TNF receptors [28]. Moreover, depletion or knock out of RIP1 has been shown to lead to enhance sensitization to TNF-induced apoptosis [29, 30]. However, in our study, Nec-1 attenuated cleavage of caspase-3, which is a marker of hepatocellular apoptosis after GalN/LPS injection. Our findings demonstrated that Nec-1 attenuates RIP1 activation, and furthermore, if we attenuate this phosphorylation, hepatocyte apoptosis may also be attenuated.

Filliol *et al*. demonstrated that RIP1 expressed on hepatocytes maintain liver homeostasis and protect against caspase-3-dependent cell death induced by TNF-α release by the Kupffer cells [31, 32]. Furthermore, RIP1 knockout exacerbates immune-mediated liver injury through apoptotic pathway [30, 33]. These suggest that RIP1 may serve a divergent role in different cell types and play a key role essential adapter in innate immune signal transduction pathways and in homeostatic maintenance of hepatic function/cell survival. Altogether, these findings imply that RIPs may function at the cross-roads of cell survival and death, which are dependent to their expression level and/or modified states. Thus, several additional points of evidence will require further advancement of our understanding of control mediation and execution of these processes in FHF.

Most studies on DAMPs have been devoted to DAMPs that are released during accidental cell death and by secondary necrotic cells following apoptosis. Relatively, few studies have investigated whether necroptosis is accompanied by release of a distinct set of DAMPs and the roles of these DAMPs in necroptosis-induced inflammation. Among them, HMGB1, calreticulin, heat shock proteins, and IL-1α are most relevant to date. HMGB1 is released actively from immune cells after acetylation and passively from dead/damaged cells induced by trauma or infection [34, 35]. RIP3-mediated necroptosis promotes the extracellular release of HMGB1 during heart and kidney I/R injury [14, 36], and released HMGB1 after red blood cell transfusion enhances susceptibility to lung inflammation and subsequent endothelial cell necroptosis [37]. IL-33, a member of IL-1 family, is proposed to be released in the functional/active form during necrotic cell death as an alarmin while it is inactivated during apoptotic cell death by caspases [38]. Rickard *et al*. reported that deletion of RIP3 prevented extracellular release of IL-33 and reduced MyD88-dependent inflammation [39]. IL-33 is expressed in hepatocytes and is regulated by natural killer T cells during Con A-induced acute liver injury, and this suggests the importance of IL-33 in the massive inflammation during FHF [40]. In liver, Nec-1 treatment attenuated hepatic IL-33 expression against Con A intoxication and protects liver inflammation and subsequent injury [41]. We indeed observed that serum release of HMGB1 and IL-33 significantly increased after GalN/LPS injection and was attenuated by Nec-1 treatment. These results suggest that prevention of necroptosis after Nec-1 administration alleviated inflammatory responses, which can be triggered by DAMPs released after cell death.

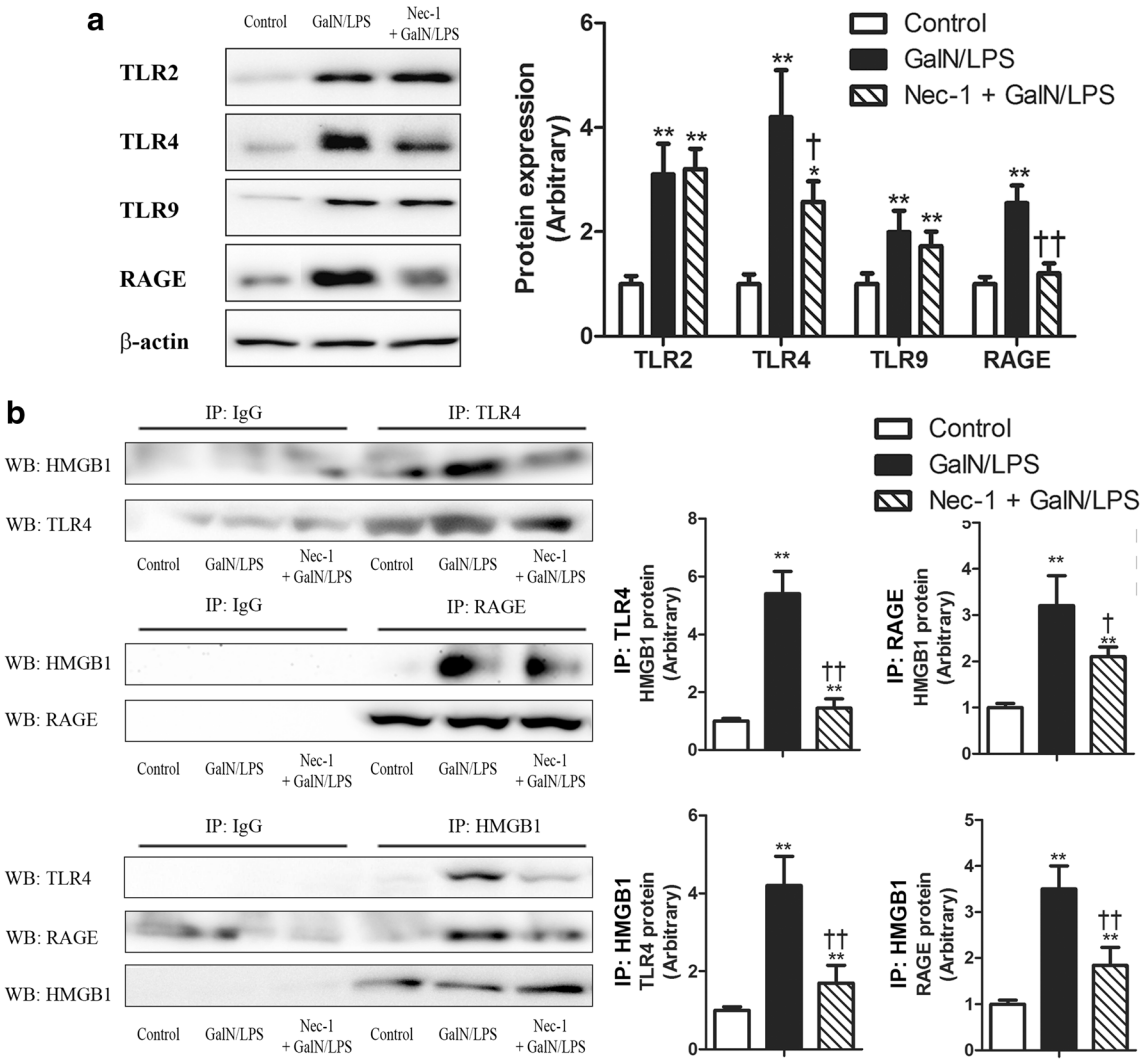

Fig. 4. Nec-1 attenuates GalN/LPS-induced increases in hepatic **a** TLR2, TLR4, TLR9, and RAGE protein expression and **b** interaction between HMGB1-TLR4 and HMGB1-RAGE. Mice were treated intraperitoneally with Nec-1 (1.8 mg/kg) or vehicle (2% DMSO in phosphate-buffered saline) at 1 h before GalN (800 mg/kg)/LPS (40 μg/kg) injection. Liver samples were obtained 3 h after GalN/LPS injection. The results are presented as mean ± S.E.M. of 8 to 10 animals per group. The *asterisk* denotes significant differences (**$P < 0.01$) *versus* the control group. The *dagger signs* denote significant differences ($^{\dagger}P < 0.05$, $^{\dagger\dagger}P < 0.01$) *versus* the GalN/LPS group.

Accumulating evidence strongly suggest that *in vivo* necroptosis is associated with an inflammatory reaction in various experimental models of inflammatory diseases [25, 42]. However, there is only limited knowledge of the molecular mechanisms involved and the role of the proinflammatory DAMPs emitted during necroptosis. Previous studies showed that stimulation of TLR3 or TLR4 triggers the recruitment of TRIF, whose RIP homotypic interaction motif (RHIM) subsequently interacts with the RHIM motif of RIP1 and RIP3 [43]. Furthermore, microglia activated through TLRs can undergo RIP3-mediated necroptosis when sensitized with pan-caspase inhibitor zVAD-fmk [44]. Interestingly, the TLR4 signaling pathway is involved in HMGB1 secretion from macrophages by a mechanism that depends on IL-1 receptor-associated kinase 4 [45], suggesting that HMGB1 might be released during TLR-mediated necroptosis. Recently, Duprez *et al.* proposed that a combination of several DAMPs released by necroptotic cells in TNF-induced systemic inflammatory response syndrome and cecal ligation and puncture-induced peritoneal sepsis might synergistically trigger sustained cytokine release and amplify the inflammatory

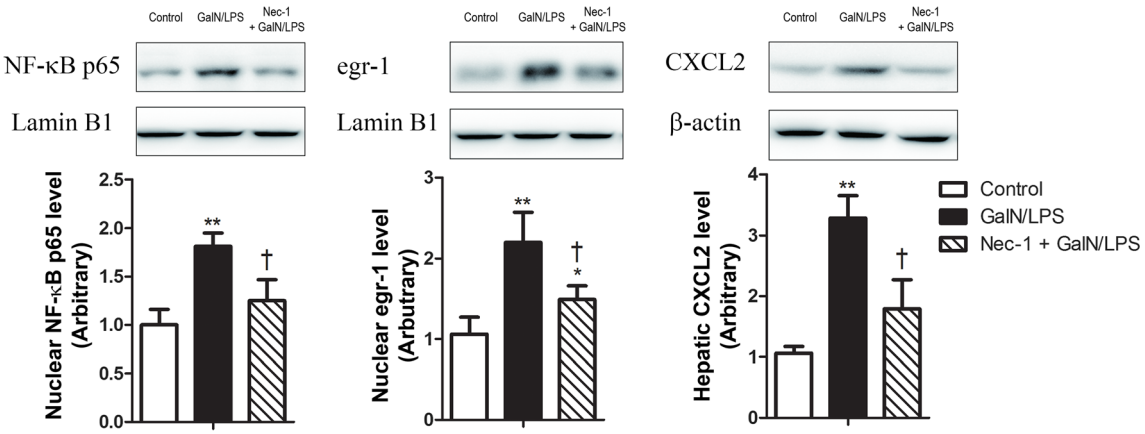

Fig. 5. Nec-1 attenuates GalN/LPS-induced increases in hepatic nuclear NF-κB p65 and egr-1 protein expression and hepatic CXCL2 protein expression. Mice were treated intraperitoneally with Nec-1 (1.8 mg/kg) or vehicle (2% DMSO in phosphate-buffered saline) at 1 h before GalN (800 mg/kg)/LPS (40 μg/kg) injection. Liver samples were obtained 3 h after GalN/LPS injection. The results are presented as mean ± S.E.M. of 8 to 10 animals per group. The *asterisk* denotes significant differences (**$P < 0.01$) from the control group. The *dagger sign* denotes significant differences ($^{\dagger}P < 0.05$) from the GalN/LPS group.

response [46]. Indeed, mitochondrial DNA can activate TLR9 and was identified as a major DAMP contributing to inflammatory responses in trauma patients developing sepsis [47]. Due to the unique vascular supply of the liver, pathogen-associated molecular patterns (PAMPs) of intestinal origin and DAMPs of hepatocyte origin collectively contribute to inflammation in a number of diseases [48]. In liver, HMGB1 act as an inflammatory cytokine, and affect hepatocyte by integrating the activities of PRRs, and particularly TLR2, TLR4, TLR9 and RAGE are subjected as a main effector [49, 50]. Although, the crucial role of TLR4 has been implicated in the development of FHF, the role of other TLRs such as TLR2 and TLR9 in FHF and linkage of necroptosis to activation of TLR in inflammatory signaling remain unclear. RAGE is a transmembrane receptor identified as a crucial mediator for amplifying and perpetuating inflammation by ligation to its ligands (*e.g.*, HMGB1, amyloid-β, and AGEs). HMGB1 acts through RAGE on macrophages [51]; however, mechanistic link between necroptosis-induced HMGB1 and RAGE is much less understood. The importance of RAGE triggering inflammatory injury has been recently emphasized as it recruits neutrophils followed by acetaminophen-induced liver necrosis [52], and blockade of RAGE through treatment of soluble RAGE-Ab in GalN/LPS-intoxicated mice attenuated hepatic microcirculatory dysfunction and hepatocellular necrosis [53]. In our study, we found a significant increase in hepatic TLR2, TLR4, TLR9, and RAGE expression. Nec-1 attenuated the increases in TLR4 and RAGE, but not TLR2 and TLR9. Although we measured TLR2, TLR4, and RAGE protein expression levels in whole liver lysates, the cellular source of PRRs has to be further highlighted. Previous reports show that hepatocytes express TLRs and are responsive to LPS, but this response is weak [54], and TLRs on Kupffer cells are considered to play major role in propagating inflammatory responses in liver. In addition, Kuhla *et al*. demonstrated that RAGE plays an important role in mediating endotoxemic liver damage [53]. Our previous study in isolated Kupffer cells and animal models using RAGE siRNA showed that Kupffer cells express RAGE and silencing RAGE by siRNA significantly attenuated production of inflammatory cytokine [55]. Collectively, TLRs and RAGE expressed on Kupffer cells play critical role mediating GalN/LPS challenge and inhibiting these receptors, particularly inhibiting TLR4 is well recognized to be beneficial in animal models [56, 57]. However, there is contradictory report that RAGE expression is mostly on liver sinusoid endothelial cells and hepatocytes, and it is poorly expressed on Kupffer cells [58], and this suggest the necessity of further study of the role of RAGE expressed on other cell population is required.

Although the full complex regulatory mechanisms of these inconsistent alterations in TLR expression have not been identified, our result indicates that the individual TLR seems to be differentially affected by necroptotic injury, and released necroptotic DAMPs may preferentially activate TLR4 and RAGE. These results are consistent with previous report that HMGB1 failed to delay ulcer healing and to promote inflammatory cytokine production in TLR4 KO and RAGE KO mice while TLR2 KO did not affect those in

experimental gastric ulcer [59]. Indeed, we demonstrated increases in the association between hepatic HMGB1-TLR4 and HMGB1-RAGE, which were attenuated by Nec-1. Consistent with these data, Nec-1 attenuated the activation of transcription factor NF-κB which regulates gene encoding proinflammatory cytokines. Furthermore, increased egr-1, a zinc-finger-transcription factor and downstream target of RAGE, and CXCL2 were attenuated by Nec-1. Taken together, our data suggest that necroptotic DAMPs may promote inflammatory response through TLR4 and RAGE signaling.

Overall, this study demonstrated that pharmacological inhibition of RIP1 prevents cell death during FHF, and this may alter the acute inflammatory responses, and we proposed their possible molecular signaling. Furthermore, our present study demonstrated that DAMPs are released by necroptotic cells and suggests the key role of DAMPs in the liver as an important mediator to the immune responses during FHF.

ACKNOWLEDGEMENTS

This research was supported by the Basic Science Research Program through the National Research Foundation of Korea (NRF) funded by the Ministry of Science, ICT, and Future Planning (NRF-2013R1A1A3008145).

COMPLIANCE WITH ETHICAL STANDARDS

Conflict of Interest. The authors declare that they have no conflict of interest.

Ethical Approval. All procedures performed in studies involving animals were in accordance with the ethical standards of the institution or practice at which the studies were conducted.

REFERENCES

1. Micheau, O., and J. Tschopp. 2003. Induction of TNF receptor I-mediated apoptosis via two sequential signaling complexes. *Cell* 114 (2): 181–190.
2. Chan, F. 2012. Fueling the flames: mammalian programmed necrosis in inflammatory diseases. *Cold Spring Harbor Perspectives in Biology* 4 (11): a008805. doi:10.1101/cshperspect.a008805.
3. Vandenabeele, P., L. Galluzzi, T. Vanden Berghe, and G. Kroemer. 2010. Molecular mechanisms of necroptosis: an ordered cellular explosion. *Nature Reviews. Molecular Cell Biology* 11 (10): 700–714. doi:10.1038/nrm2970.
4. Degterev, A., Z. Huang, M. Boyce, Y. Li, P. Jagtap, N. Mizushima, G.D. Cuny, T.J. Mitchison, M.A. Moskowitz, and J. Yuan. 2005. Chemical inhibitor of nonapoptotic cell death with therapeutic potential for ischemic brain injury. *Nature Chemical Biology* 1 (2): 112–119. doi:10.1038/nchembio711.
5. Li, Y., X. Yang, C. Ma, J. Qiao, and C. Zhang. 2008. Necroptosis contributes to the NMDA-induced excitotoxicity in rat's cultured cortical neurons. *Neuroscience Letters* 447 (2–3): 120–123. doi:10.1016/j.neulet.2008.08.037.
6. Oerlemans, M.I., J. Liu, F. Arslan, K. den Ouden, B.J. van Middelaar, P.A. Doevendans, and J.P. Sluijter. 2012. Inhibition of RIP1-dependent necrosis prevents adverse cardiac remodeling after myocardial ischemia-reperfusion in vivo. *Basic Research in Cardiology* 107 (4): 270–278. doi:10.1007/s00395-012-0270-8.
7. Xu, X., C.C. Chua, J. Kong, R.M. Kostrzewa, U. Kumaraguru, R.C. Hamdy, and B.H. Chua. 2007. Necrostatin-1 protects against glutamate-induced glutathione depletion and caspase-independent cell death in HT-22 cells. *Journal of Neurochemistry* 103 (5): 2004–2014. doi:10.1111/j.1471- 4159.2007.04884.x.
8. Jouan-Lanhouet, S., M.I. Arshad, C. Piquet-Pellorce, C. Martin-Chouly, G. Le Moigne-Muller, F. Van Herreweghe, N. Takahashi, et al. 2012. TRAIL induces necroptosis involving RIPK1/RIPK3-dependent PARP-1 activation. *Cell Death and Differentiation* 19: 2003–2014. doi:10.1038/cdd.2012.90.
9. Zhou, Y., W. Dai, C. Lin, F. Wang, L. He, M. Shen, P. Chen, et al. 2013. Protective effects of necrostatin-1 against concanavalin A-induced acute hepatic injury in mice. *Mediators of Inflammation* 2013: 706156. doi:10.1155/2013/706156.
10. Zhang, Y.F., W. He, C. Zhang, X.J. Liu, Y. Lu, H. Wang, Z.H. Zhang, X. Chen, and D.X. Xu. 2014. Role of receptor interacting protein (RIP)1 on apoptosis-inducing factor-mediated necroptosis during acetaminophen-evoked acute liver failure in mice. *Toxicology Letters* 225 (3): 445–453. doi:10.1016/j.toxlet.2014.01.005.
11. Takemoto, K., E. Hatano, K. Iwaisako, M. Takeiri, N. Noma, S. Ohmae, K. Toriguchi, et al. 2014. Necrostatin-1 protects against reactive oxygen species (ROS)-induced hepatotoxicity in acetaminophen-induced acute liver failure. *FEBS Open Bio* 4 (1): 777–787. doi:10.1016/j.fob.2014.08.007.
12. Ramachandran, A., M.R. McGill, Y. Xie, H.M. Ni, W.X. Ding, and H. Jaeschke. 2013. Receptor interacting protein kinase 3 is a critical early mediator of acetaminophen-induced hepatocyte necrosis in mice. *Hepatology* 58 (6): 2099–2108. doi:10.1002/hep.26547.
13. Roychowdhury, S., M.R. McMullen, S.G. Pisano, X. Liu, and L.E. Nagy. 2013. Absence of receptor interacting protein kinase 3 prevents ethanol-induced liver injury. *Hepatology* 57 (5): 1773–1783. doi:10.1002/hep.26200.
14. Lau, A., S. Wang, J. Jiang, A. Haig, A. Pavlosky, A. Linkermann, Z.X. Zhang, and A.M. Jevnikar. 2013. RIPK3-mediated necroptosis promotes donor kidney inflammatory injury and reduces allograft survival. *American Journal of Transplantation* 13 (11): 2805–2818. doi:10.1111/ajt.12447.
15. Murakami, Y., H. Matsumoto, M. Roh, A. Giani, K. Kataoka, Y. Morizane, M. Kayama, et al. 2014. Programmed necrosis, not apoptosis, is a key mediator of cell loss and DAMP-mediated inflammation in dsRNA-induced retinal degeneration. *Cell Death and Differentiation* 21 (2): 270–277. doi:10.1038/cdd.2013.109.
16. He, S., Y. Liang, F. Shao, and X. Wang. 2011. Toll-like receptors activate programmed necrosis in macrophages through a receptor-interacting kinase-3-mediated pathway. *Proceedings of the National*

Academy of Sciences of the United States of America 108 (50): 20054–20059. doi:10.1073/pnas.1116302108.

17. Kaczmarek, A., P. Vandenabeele, and D.V. Krysko. 2013. Necroptosis: the release of damage-associated molecular patterns and its physiological relevance. *Immunity* 38 (2): 209–223. doi:10.1016/j.immuni.2013.02.003.
18. Zeng, S., H. Dun, N. Ippagunta, R. Rosario, Q.Y. Zhang, J. Lefkowitch, S.F. Yan, A.M. Schmidt, and J.C. Emond. 2009. Receptor for advanced glycation end product (RAGE)-dependent modulation of early growth response-1 in hepatic ischemia/reperfusion injury. *Journal of Hepatology* 50 (5): 929–936. doi:10.1016/j.jhep.2008.11.022.
19. Mocarski, E.S., H. Guo, and W.J. Kaiser. 2015. Necroptosis: the Trojan horse in cell autonomous antiviral host defense. *Virology* 479–480: 160–166. doi:10.1016/j.virol.2015.03.016.
20. Wu, J., Z. Huang, J. Ren, Z. Zhang, P. He, Y. Li, J. Ma, et al. 2013. MLKL knockout mice demonstrate the indispensable role of MLKL in necroptosis. *Cell Research* 23 (8): 994–1006. doi:10.1038/cr.2013.91.
21. Kim, S.J., J.K. Kim, D.U. Lee, J.H. Kwak, and S.M. Lee. 2010. Genipin protects lipopolysaccharide-induced apoptotic liver damage in D-galactosamine-sensitized mice. *European Journal of Pharmacology* 635 (1–3): 188–193. doi:10.1016/j.ejphar.2010.03.007.
22. Murphy, J. M., and J. E. Vince. 2015. Post-translational control of RIPK3 and MLKL mediated necroptotic cell death. *F1000Research* 4. doi:10.12688/f1000research.7046.1.
23. Remijsen, Q., V. Goossens, S. Grootjans, C. Van den Haute, N. Vanlangenakker, Y. Dondelinger, R. Roelandt, et al. 2014. Depletion of RIPK3 or MLKL blocks TNF-driven necroptosis and switches towards a delayed RIPK1 kinase-dependent apoptosis. *Cell Death and Disease* 5: e1004. doi:10.1038/cddis.2013.531.
24. Murphy, J.M., P.E. Czabotar, J.M. Hildebrand, I.S. Lucet, J.G. Zhang, S. Alvarez-Diaz, R. Lewis, et al. 2016. The pseudokinase MLKL mediates necroptosis via a molecular switch mechanism. *Immunity* 39 (3): 443–453. doi:10.1016/j.immuni.2013.06.018.
25. Afonso, M.B., P.M. Rodrigues, T. Carvalho, M. Caridade, P. Borralho, H. Cortez-Pinto, R.E. Castro, and C.M.P. Rodrigues. 2015. Necroptosis is a key pathogenic event in human and experimental murine models of non-alcoholic steatohepatitis. *Clinical Science* 129 (8): 721–739. doi:10.1042/CS20140732.
26. Morikawa, A., T. Sugiyama, Y. Kato, N. Koide, G.Z. Jiang, K. Takahashi, Y. Tamada, and T. Yokochi. 1996. Apoptotic cell death in the response of D-galactosamine-sensitized mice to lipopolysaccharide as an experimental endotoxic shock model. *Infection and Immunity* 64 (3): 734–738.
27. Bahjat, F.R., V.R. Dharnidharka, K. Fukuzuka, L. Morel, J.M. Crawford, M.J. Clare-Salzler, and L.L. Moldawer. 2000. Reduced susceptibility of nonobese diabetic mice to TNF-alpha and D-galactosamine-mediated hepatocellular apoptosis and lethality. *Journal of Immunology* 165 (11): 6559–6567.
28. Nowak, M., G.C. Gaines, J. Rosenberg, R. Minter, F.R. Bahjat, J. Rectenwald, S.L. MacKay, C.K. Edwards, and L.L. Moldawer. 2000. LPS-induced liver injury in D-galactosamine-sensitized mice requires secreted TNF-alpha and the TNF-p55 receptor. *American Journal of Physiology. Regulatory, Integrative and Comparative Physiology* 278 (5): 1202–1209.
29. Takahashi, N., L. Vereecke, M.J. Bertrand, L. Duprez, S.B. Berger, T. Divert, A. Gonçalves, et al. 2014. RIPK1 ensures intestinal homeostasis by protecting the epithelium against apoptosis. *Nature* 513 (7516): 95–99. doi:10.1038/nature13706.
30. Suda, J., L. Dara, L. Yang, M. Aghajan, Y. Song, N. Kaplowitz, and Z.X. Liu. 2016. Knockdown of RIPK1 markedly exacerbates murine immune-mediated liver injury through massive apoptosis of hepatocytes, independent of necroptosis and inhibition of NF-κB. *Journal of Immunology* 197 (8): 3120–3129. doi:10.4049/jimmunol.1600690.
31. Filliol, A., C. Piquet-Pellorce, C. Raguénès-Nicol, S. Dion, M. Farooq, C. Lucas-Clerc, P. Vandenabeele, M.J.M. Bertrand, J. Le Seyec, and M. Samson. 2017. RIPK1 protects hepatocytes from Kupffer cells-mediated TNF-induced apoptosis in mouse models of PAMP-induced hepatitis. *Journal of Hepatology* 66 (6): 1205–1213. doi:10.1016/j.jhep.2017.01.005.
32. Filliol, A., C. Piquet-Pellorce, J. Le Seyec, M. Farooq, V. Genet, C. Lucas-Clerc, J. Bertin, et al. 2016. RIPK1 protects from TNF-α-mediated liver damage during hepatitis. *Cell death and disease* 7 (11): e2462. doi:10.1038/cddis.2016.362.
33. Schneider, A.T., J. Gautheron, M. Feoktistova, C. Roderburg, S.H. Loosen, S. Roy, F. Benz, et al. 2017. RIPK1 suppresses a TRAF2-dependent pathway to liver cancer. *Cancer Cell* 31 (1): 94–109. doi:10.1016/j.ccell.2016.11.009.
34. Chen, G., J. Li, M. Ochani, B. Rendon-Mitchell, X. Qiang, S. Susarla, L. Ulloa, et al. 2004. Bacterial endotoxin stimulates macrophages to release HMGB1 partly through CD14- and TNF-dependent mechanisms. *Journal of Leukocyte Biology* 76 (5): 994–1001. doi:10.1189/jlb.0404242.
35. Gardella, S., C. Andrei, D. Ferrera, L.V. Lotti, M.R. Torrisi, M.E. Bianchi, and A. Rubartelli. 2002. The nuclear protein HMGB1 is secreted by monocytes via a non-classical, vesicle-mediated secretory pathway. *EMBO Reports* 3 (10): 995–1001. doi:10.1093/embo-reports/kvf198.
36. Pavlosky, A., A. Lau, Y. Su, D. Lian, X. Huang, Z. Yin, A. Haig, A.M. Jevnikar, and Z.X. Zhang. 2014. RIPK3-mediated necroptosis regulates cardiac allograft rejection. *American Journal of Transplantation* 14 (8): 1778–1790. doi:10.1111/ajt.12779.
37. Qing, D.Y., D. Conegliano, M.G. Shashaty, J. Seo, J.P. Reilly, G.S. Worthen, D. Huh, N.J. Meyer, and N.S. Mangalmurti. 2014. Red blood cells induce necroptosis of lung endothelial cells and increase susceptibility to lung inflammation. *American Journal of Respiratory and Critical Care Medicine* 190 (11): 1243–1254. doi:10.1164/rccm.201406-1095OC.
38. Lefrancais, E., and C. Cayrol. 2012. Mechanisms of IL-33 processing and secretion: differences and similarities between IL-1 family members. *European Cytokine Network* 23 (4): 120–127. doi:10.1684/ecn.2012.0320.
39. Rickard, J.A., J.A. O'Donnell, J.M. Evans, N. Lalaoui, A.R. Poh, T. Rogers, J.E. Vince, et al. 2014. RIPK1 regulates RIPK3-MLKL-driven systemic inflammation and emergency hematopoiesis. *Cell* 157 (5): 1175–1188. doi:10.1016/j.cell.2014.04.019.
40. Arshad, M.I., C. Piquet-Pellorce, and M. Samson. 2012. IL-33 and HMGB1 alarmins: sensors of cellular death and their involvement in liver pathology. *Liver International* 32 (8): 1200–1210. doi:10.1111/j.1478-3231.2012.02802.x.
41. Arshad, M.I., C. Piquet-Pellorce, A. Filliol, A. L'Helgoualc'h, C. Lucas-Clerc, S. Jouan-Lanhouet, M.T. Dimanche-Boitrel, and M. Samson. 2015. The chemical inhibitors of cellular death, PJ34 and necrostatin-1, down-regulate IL-33 expression in liver. *Journal of Molecular Medicine* 93 (8): 867–878. doi:10.1007/s00109-015-1270-6.
42. Liu, Z.Y., B. Wu, Y.S. Guo, Y.H. Zhou, Z.G. Fu, B.Q. Xu, J.H. Li, et al. 2015. Necrostatin-1 reduces intestinal inflammation and colitis-associated tumorigenesis in mice. *American Journal of Cancer Research* 5 (10): 3174–3185.
43. Humphries, F., S. Yang, B. Wang, and P.N. Moynagh. 2015. RIP kinases: key decision makers in cell death and innate immunity. *Cell Death and Differentiation* 22 (2): 225–236. doi:10.1038/cdd.2014.126.

44. Kim, S.J., and J. Li. 2013. Caspase blockade induces RIP3-mediated programmed necrosis in Toll-like receptor-activated microglia. *Cell death and disease* 4: e716. doi:10.1038/cddis.2013.238.
45. Wang, F., Z. Lu, M. Hawkes, H. Yang, K.C. Kain, and W.C. Liles. 2010. Fas (CD95) induces rapid, TLR4/IRAK4-dependent release of pro-inflammatory HMGB1 from macrophages. *Journal of Inflammation* 7: 30. doi:10.1186/1476-9255-7-30.
46. Duprez, L., N. Takahashi, F. Van Hauwermeiren, B. Vandendriessche, V. Goossens, T. Vanden Berghe, W. Declercq, C. Libert, A. Cauwels, and P. Vandenabeele. 2011. RIP kinase-dependent necrosis drives lethal systemic inflammatory response syndrome. *Immunity* 35 (6): 908–918. doi:10.1016/j.immuni.2011.09.020.
47. Zhang, Q., M. Raoof, Y. Chen, Y. Sumi, T. Sursal, W. Junger, K. Brohi, K. Itagaki, and C.J. Hauser. 2010. Circulating mitochondrial DAMPs cause inflammatory responses to injury. *Nature* 464 (7285): 104–107. doi:10.1038/nature08780.
48. Brenner, C., L. Galluzzi, O. Kepp, and G. Kroemer. 2013. Decoding cell death signals in liver inflammation. *Journal of Hepatology* 59 (3): 583–594. doi:10.1016/j.jhep.2013.03.033.
49. Chen, R., W. Hou, Q. Zhang, R. Kang, X.G. Fan, and D. Tang. 2013. Emerging role of high-mobility group box 1 (HMGB1) in liver diseases. *Molecular Medicine* 19: 357–366. doi:10.2119/molmed.2013.00099.
50. Wang, H., O. Bloom, M. Zhang, J.M. Vishnubhakat, M. Ombrellino, J. Che, A. Frazier, et al. 1999. HMG-1 as a late mediator of endotoxin lethality in mice. *Science* 285 (5425): 248–251. doi:10.1126/science.285.5425.248.
51. Xu, J., Y. Jiang, J. Wang, X. Shi, Q. Liu, Z. Liu, Y. Li, et al. 2014. Macrophage endocytosis of high mobility group box 1 triggers pyroptosis. *Cell Death and Differentiation* 21 (8): 1229–1239. doi:10.1038/cdd.2014.40.
52. Huebener, P., J.P. Pradere, C. Hernandez, G.Y. Gwak, J.M. Caviglia, X. Mu, J.D. Loike, R.E. Jenkins, D.J. Antoine, and R.F. Schwabe. 2015. The HMGB1/RAGE axis triggers neutrophil-mediated injury amplification following necrosis. *Journal of Clinical Investigation* 125 (2): 539–550. doi:10.1172/JCI76887.
53. Kuhla, A., J. Norden, K. Abshagen, M.D. Menger, and B. Vollmar. 2013. RAGE blockade and hepatic microcirculation in experimental endotoxaemic liver failure. *British Journal of Surgery* 100 (9): 1229–1239. doi:10.1002/bjs.9188.
54. Matsumura, T., A. Ito, T. Takii, H. Hayashi, and K. Onozaki. 2000. Endotoxin and cytokine regulation of toll-like receptor (TLR) 2 and TLR4 gene expression in murine liver and hepatocytes. *Journal of Interferon & Cytokine Research* 20 (10): 915–921. doi:10.1089/10799900050163299.
55. Cho, H.I., J.M. Hong, J.W. Choi, H.S. Choi, J.H. Kwak, D.W. Lee, S.K. Lee, and S.M. Lee. 2015. β-Caryophyllene alleviates D-galactosamine and lipopolysaccharide-induced hepatic injury through suppression of the TLR4 and RAGE signaling pathways. *European Journal of Pharmacology* 764: 613–621. doi:10.1016/j.ejphar.2015.08.001.
56. Kitazawa, T., T. Tsujimoto, H. Kawaratani, and H. Fukui. 2010. Salvage effect of E5564, Toll-like receptor 4 antagonist on D-galactosamine and lipopolysaccharide-induced acute liver failure in rats. *Journal of Gastroenterology and Hepatology* 25 (5): 1009–1012. doi:10.1111/j.1440-1746.2009.06145.x.
57. Ben Ari, Z., O. Avlas, O. Pappo, V. Zilbermints, Y. Cheporko, L. Bachmetov, R. Zemel, et al. 2012. Reduced hepatic injury in Toll-like receptor 4-deficient mice following D-galactosamine/lipopolysaccharide-induced fulminant hepatic failure. *Cellular Physiology and Biochemistry* 29 (1–2): 41–50. doi:10.1159/000337585.
58. Ott, C., K. Jacobs, E. Haucke, A. Navarrete Santos, T. Grune, and A. Simm. 2014. Role of advanced glycation end products in cellular signaling. *Redox Biology* 2: 411–429. doi:10.1016/j.redox.2013.12.016.
59. Nadatani, Y., T. Watanabe, T. Tanigawa, F. Ohkawa, S. Takeda, A. Higashimori, M. Sogawa, et al. 2013. High-mobility group box 1 inhibits gastric ulcer healing through Toll-like receptor 4 and receptor for advanced glycation end products. *PloS One* 8 (11): e80130. doi:10.1371/journal.pone.0080130.